deviation (Fig. 2). We defined the rotating angle of the carpus around each of the 3 axes as the range of wrist motion.

Evaluation of the Contribution Ratio

We also evaluated the individual contributions of radiocarpal and midcarpal motion to the total amount of wrist motion. We defined *contribution ratio* as the percentage of the range of radiocarpal motion or midcarpal motion relative to the total amount of wrist motion. In this study, the contribution ratio was investigated only in the flexion-extension plane.

Statistical Analysis

All data were expressed as the mean with the standard deviation. Quantitative comparison of results between the control group and the RA group was performed using standard statistical formulas based on the Mann-Whitney U test. Results were deemed to be significant if $p < .05$.

RESULTS

Rheumatoid Arthritis Versus Normal

In the rheumatoid wrists, the average of total amount of wrist motion in the flexion-extension plane was 59° ± 20. The average range of radiocarpal motion in the flexion-extension plane was 27° ± 15 and that of midcarpal motion was 32° ± 17. In the normal wrists, the average of total amount of wrist motion in the flexion-extension plane was 111° ± 15. The average range of radiocarpal motion in the flexion-extension plane was 63° ± 14° and that of midcarpal motion was 47° ± 8. The ranges of radiocarpal motion ($p < .01$) and midcarpal motion ($p < .01$) in the flexion-extension plane in RA wrists were significantly less than normal as expected (Table 2). The average contribution ratios of radiocarpal and midcarpal joint in the flexion-extension plane were 46% and 54%, respectively, in RA wrists and 57% and 43%, respectively, in normal wrists (Fig. 3). On average, the midcarpal joint tended to have a greater contribution in the flexion-extension plane in RA wrists compared with normal wrists, even though the difference was not significant ($p = .179$).

Regarding the out of the plane motion of the wrists, the average of total amount of out of the plane motion (P/S) in RA was 8° ± 11 in supination during flexion motion of the wrist. The average range of out of the plane motion (P/S) in the radiocarpal joint was 5° ± 7 and that in the midcarpal joint was 2° ± 8 in supination during flexion motion of the wrists. In the normal wrists, the average of total amount of out of the plane motion (P/S) was 8° ± 13 in pronation during flexion motion of the wrists. The average range of out of the plane motion (P/S) in the radiocarpal joint was 3° ± 6 and that in the midcarpal joint was 4° ± 9 in pronation during flexion motion of the wrists. Consequently, during flexion motion of the wrists, the radiocarpal joint ($p < .01$) and the whole wrist joint, that is, the total for the radiocarpal and midcarpal joints ($p < .01$), significantly supinated in RA wrists compared with normal (Table 2).

The average of total amount of out of the plane motion (RD/UD) in RA was 5° ± 8 in ulnar deviation during flexion motion of the wrists. The average of out of the plane motion (RD/UD) in the radiocarpal joint was 1° ± 7 and that in the midcarpal joint was 4° ± 8 in ulnar deviation during flexion motion of the wrists. In the normal wrists, the average of total amount of out of the plane motion (RD/UD) was 8° ± 13 in radial deviation during flexion motion of the wrists. The average range of out of the plane motion (RD/UD) in the radiocarpal joint was 4° ± 8 and that in the midcarpal joint was 4° ± 8 in radial deviation during flexion motion of the wrists. Consequently, during flexion motion of the wrists, the midcarpal joint ($p < .05$) and the whole wrist joint, that is, the total for the radiocarpal and midcarpal joints ($p < .01$), significantly deviated ulnarly in RA wrists compared with normal (Table 2).

Stable Form Versus Unstable Form of RA

We classified the 30 rheumatoid wrists into 19 cases of stable form of disease and 11 cases of unstable form. The average of total ulnar translocation after onset of RA was 4.1 mm in the stable form and 10.7 mm in the unstable form; these values are consistent with the radiographic parameters described by Simmen and Huber (Table 1).[1] The average of total loss of carpal height ratio after onset of RA was 0.12 in the stable form and 0.28 in the unstable form; these values are also consistent with the radiographic parameters described by Simmen and Huber (Table 1).[1] Among the 11 wrists in the unstable form of disease, 7 showed S-L dissociation. In contrast, S-L dissociation was not found among the 19 wrists in the stable form of disease.

The range of radiocarpal and midcarpal motions in the flexion-extension plane varied greatly among cases in the stable form of disease (Fig. 4). In contrast, the range in cases of the unstable form was relatively constant; in 8 of the 11 wrists in unstable form, the midcarpal motion in the flexion-extension plane was greater than radiocarpal motion (Figs. 4, 5). Only 3 cases of the unstable form had greater motion in the radiocarpal joint than in the midcarpal joint (Fig. 4). The average ranges of radiocarpal and midcarpal motion in the flexion-extension plane were 31° ± 16 and 28° ± 15, respectively, in the stable form, and 20° ± 12 and 38° ± 19, respectively, in the unstable form. In the radiocarpal joint, the range of motion of the unstable form in the flexion-extension plane was significantly less than that of the stable form ($p < .05$), whereas in the midcarpal joint, there was no significant difference ($p < .05$) between the 2 groups (Table 3). The average contribution ratios of radiocarpal and midcarpal joint in the flexion-extension plane were 53% and 47%, respectively, in the stable form and 33% and 67%, respectively, in the unstable form (Fig. 6). In the midcarpal joint, the contribution ratio of the unstable-form group in the flexion-extension plane was significantly greater than that of the stable-form group ($p < .05$).

Regarding out of the plane motion (P/S) of the rheumatoid wrists, during flexion motion of the wrists, the

TABLE 2: Kinematic Data During Flexion Motion of the Wrist: RA Versus Normal Wrists

	Range of Motion During the Flexion Motion of the Wrists (°)								
	In the Flexion-Extension Plane Motion			Out of the Flexion-Extension Plane Motion					
	Flexion (+)/Extension (–)			Pronation (+)/Supination (–)			Ulnar (+)/Radial (–) Deviation		
	Radiocarpal Motion	Midcarpal Motion	Total Amount of Motion	Radiocarpal Motion	Midcarpal Motion	Total Amount of Motion	Radiocarpal Motion	Midcarpal Motion	Total Amount of Motion
Normal (n = 10)									
Average	63	47	111	3	4	8	–4	–4	–8
SD	14	8	15	6	9	13	8	8	13
RA (n = 30)									
Average	27**	32**	59**	–5**	–2	–8**	1	4*	5**
SD	15	17	20	7	8	11	7	8	8

*$p < .05$, **$p < .01$ versus normal.

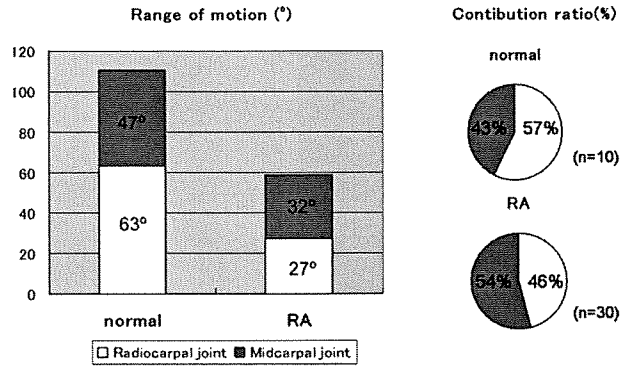

FIGURE 3: Average range of motion and contribution ratios of the radiocarpal and midcarpal joint in the flexion-extension plane in normal and RA wrists. The contribution ratio is the percentage contribution of radiocarpal or midcarpal motion relative to the total amount of wrist motion.

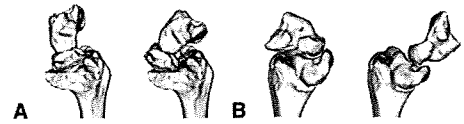

FIGURE 5: Flexion-extension motions of the lunate and capitate relative to the radius in the stable and unstable forms of RA wrists, viewed from the ulnar side. **A** Representative case of the stable form of RA, shown in Figure 1A, in which the range of motion in the flexion-extension plane was 40° in the radiocarpal joint and 5° in the midcarpal joint (Video 1, a 3-dimensional animation of a representative case of the stable form of RA wrist, may be viewed at the *Journal's* Web site, www.jhandsurg.org). **B** Representative case of the unstable form of RA, shown in Figure 1B, in which the range of motion in the flexion-extension plane was 37° in the radiocarpal joint and 83° in the midcarpal joint (Video 2, a 3-dimensional animation of a representative case of the unstable form of RA wrist, may be viewed at the *Journal's* Web site, www.jhandsurg.org).

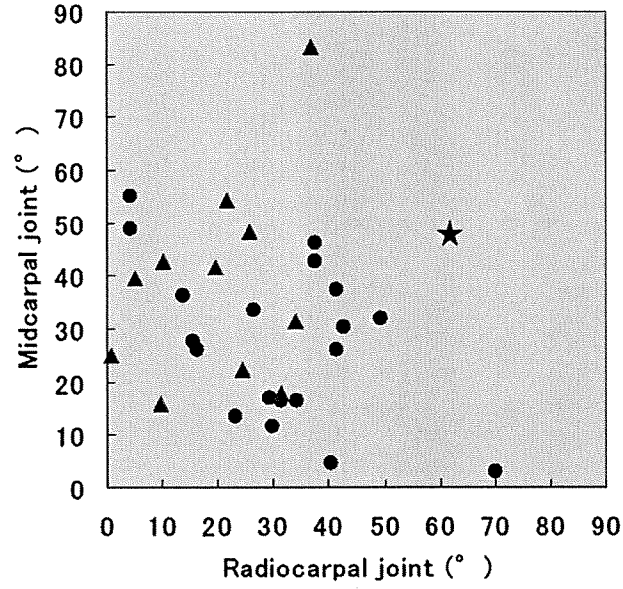

FIGURE 4: Scattering diagram of the range of the radiocarpal and midcarpal motion in the flexion-extension plane in stable and unstable forms of RA wrists and in normal wrists: ●, stable form of RA (19 cases); ▲, unstable form of RA (11 cases); ★, average range of motion in 10 normal wrists (63° in the radiocarpal joint and 47° in the midcarpal joint).

midcarpal joint ($p < .05$) and the whole wrist joint, that is, the total for the radiocarpal and midcarpal joints ($p < .01$), significantly supinated in the unstable-form group compared with the stable-form group. Regarding out of the plane motion (RD/UD), we found no significant difference ($p < .05$) between the 2 groups (Table 3).

DISCUSSION

Kinematic evaluation of rheumatoid wrists by x-ray has been difficult because of the complicated and overlapping shapes of the carpal bones. In the current study, we quantitatively evaluated the amount of radiocarpal and midcarpal motion in the flexion-extension plane of the rheumatoid wrists using 3-D CT. We also elucidated the relationship between the contribution of midcarpal motion to the total amount of wrist motion in the flexion-extension plane and the radiographic subtypes of RA.

We found that the contribution of midcarpal motion to the total amount of wrist motion in the flexion-extension plane was significantly greater in the unstable form than in the stable form of RA (Table 3 and Fig. 6). This result may seem counterintuitive because of the radiographic appearance of the unstable form of RA in which all parts of the wrist joints are severely damaged. We speculate that our results can be accounted for mainly by stronger skeletal constraints in the midcarpal joint than in the radiocarpal joint. The midcarpal joint has its own self-stabilizing mechanism; when the trapezium is axially loaded against the scaphoid, the flexion moment by the scaphoid is constrained by the extension moment experienced by the triquetrum, and stable equilibrium is achieved.[19] Moreover, the midcarpal joint is proved to have an adaptive mechanism whereby the concave and convex joint surfaces allow preservation of articular congruity.[19] On the other hand, the stability of the radiocarpal joint depends on ligamentous constraints. In the radiocarpal joint, the carpal bones tend to slide ulno-palmarward on the sloping plane of the distal radius, and the displacement is resisted by the palmar and dorsal radiotriquetral and palmar RL ligaments.[22] It is likely that the radiocarpal joint in which joint stability depends on ligamentous constraints easily loses its stability, particularly in the unstable form of RA.

Scapholunate dissociation can be associated with RA wrist by the multiple laxities of ligaments including the dorsal scapholunate ligament, especially in the unstable form of RA. In the current study, S-L dissociation occurred in 7 of 11 wrists in the unstable form of RA; however, it did not occur in any of the 19 wrists in the stable form. This may have the relationship to our results that the range of

TABLE 3: Kinematic Data During Flexion Motion of the Wrist: Stable Versus Unstable Forms of RA

	Range of Motion During the Flexion Motion of the Rheumatoid Wrists (°)								
	In the Flexion-Extension Plane Motion			Out of the Flexion-Extension Plane Motion					
	Flexion (+)/Extension (–)			Pronation (+)/Supination (–)			Ulnar (+)/Radial (–) Deviation		
	Radiocarpal Motion	Midcarpal Motion	Total Amount of Motion	Radiocarpal Motion	Midcarpal Motion	Total Amount of Motion	Radiocarpal Motion	Midcarpal Motion	Total Amount of Motion
Stable form (n = 19)									
Average	31	28	59	–3	0	–3	2	3	5
SD	16	15	15	5	7	9	5	7	7
Unstable form (n = 11)									
Average	20*	38	58	–9	–7*	–16**	1	6	7
SD	12	19	25	9	7	10	8	9	9

*$p < .05$, **$p < .01$ versus stable form.

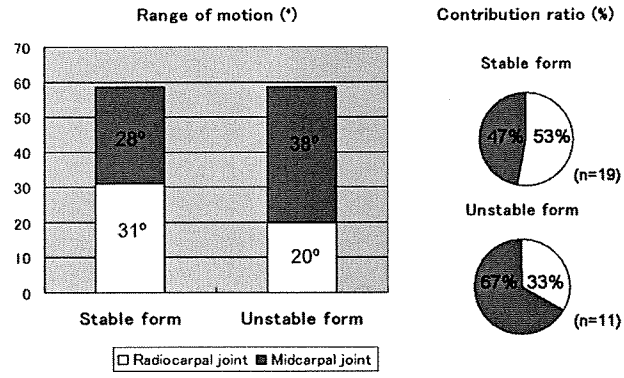

FIGURE 6: Average range of motion and the contribution ratios of the radiocarpal and midcarpal joints in the flexion-extension plane in the stable and unstable forms of RA wrists. The contribution ratio is the percentage of the contribution of the radiocarpal motion or midcarpal motion relative to the total amount of wrist motion.

radiocarpal motion in the unstable form in the flexion-extension plane was significantly less than that in the stable form. In the normal wrists, if the interosseous ligament between scaphoid and lunate is disrupted, the scaphoid tends to flex and the lunate tends to extend and the congruity of the radiocarpal joint is lost.[23] These tendencies may lead to the loss of the range of radiocarpal motion.

Regarding the motion of the wrists outside the flexion-extension plane, we found RA wrists significantly deviated ulnarly during flexion motion compared with normal (Table 2). This may be related to the unique motion patterns of the midcarpal joint. It has been reported that the essential plane of motion of the midcarpal joint is oblique to the anatomic planes, which corresponds with extension with radial deviation and flexion with ulnar deviation—the so-called dart-throwing motion.[19] Under the severe destruction of the radiocarpal joint in RA, especially in the unstable form, it is possible that the preserved midcarpal function facilitates the dart-throwing motion rather than the pure flexion-extension motion. This dart-throwing motion seems to be helpful for patients with RA because the oblique motion is used in performing many tasks of daily living such as hair combing, washcloth wringing, shoe tying, and can-opening.[24,25]

Most clinical reports have asserted that osseous procedures such as partial fusions of compartments of the joint are recommended to stabilize wrists with RA.[1] It has been suggested that RL arthrodesis is indicated only in the middle stage of the osteoarthritis type of RA and that other types such as the unstable form of RA may be better treated by total wrist arthrodesis.[3] However, reconsideration is needed because total wrist arthrodesis involves considerable loss of wrist function. Borisch and Haussmann[10] reported that the RL arthrodesis was able to reestablish the midcarpal joint and that the carpus showed an amazing capacity of adaptation. Ishikawa et al[11] suggested that radiocarpal fusion resulted in good stability with preservation of motion despite radiographic progression of the disease. Our results showing that the midcarpal motion in the unstable form of RA was better preserved than previously thought may support more positive application of RL arthrodesis in certain cases with the unstable form of RA. However, our results do not predict wrist function perfectly after RL arthrodesis in ongoing disease, because previous researchers reported that although the midcarpal joint space was generally preserved after radiocarpal arthrodesis, some wrists lost the joint space and became stiff.[9,11]

The current study has some limitations. The most important limitation is that we compared data on patients with RA based on CT images with data on normal volunteers based on MRI. However, we quantified the range of joint motion as the rotational angle of the carpus relative to a reference system established in the radius. The way in which the images are acquired may not affect the overall results if it is under the accuracy of volume-based registration. A second limitation of this study is that the patients with RA wrists were not fully matched for age and gender with the normal-wrist volunteers. The results might have been different if these demographic parameters of the study groups were identical. A further limitation is that during image acquisition, we were unable to use the position-holding device in the RA patients to maintain the neutral, maximum flexion, and extension positions because of symptomatic pain and wrist deformity. Because the patients used their own muscle power to hold their wrists in position, the positions recorded may not have been precisely maximum flexion and maximum extension.

Nevertheless, the results of this study may be useful in establishing a treatment plan in advanced cases of RA. Even some cases in the stable form of RA wrist may be treated by RL fusion, particularly the cases in which the midcarpal joint space is not visible on x-ray but the midcarpal motion is preserved under the 3-D investigation. Based on our findings of the preservation of a great amount of motion at the midcarpal joint in rheumatoid patients with symptomatic wrists, we believe that our study rationally supports the application of RL arthrodesis rather than total wrist arthrodesis as treatment in appropriate RA patients.

REFERENCES

1.Simmen BR, Huber H. The rheumatoid wrist: a new classification related to the type of the natural course and its consequences for surgical therapy. In: Simmen BR, Hagena FW, eds. The wrist in rheumatoid arthritis. Rheumatology. Basel: Karger, 1992:13–25.

2.Flury MP, Herren DB, Simmen BR. Rheumatoid arthritis of the wrist. Classification related to the natural course. Clin Orthop 1999;366:72–77.

3.Della Santa D, Chamay A. Radiological evolution of the rheumatoid wrist after radio-lunate arthrodesis. J Hand Surg 1995;20B:146–154.

4.Chamay A, Della Santa D, Vilaseca A. Radiolunate arthrodesis. Factor of stability for the rheumatoid wrist. Ann Chir Main 1983;2:5–17.

5.Linscheid RL, Dobyns JH. Radiolunate arthrodesis. J Hand Surg 1985;10A:821–829.

6.Stanley JK, Boot DA. Radiolunate arthrodesis. J Hand Surg 1989;14B:283–287.
7.Ishikawa H, Hanyu T, Saito H, Takahashi H. Limited arthrodesis for the rheumatoid wrist. J Hand Surg 1992;17A: 1103–1109.
8.Halikis MN, Colello-Abraham K, Taleisnik J. Radiolunate fusion. The forgotten partial arthrodesis. Clin Orthop 1997; 341:30–35.
9.Doets HC, Raven EEJ. Radiolunate arthrodesis. A procedure for stabilizing and preserving mobility in the arthritic wrist. J Bone Joint Surg 1999;81B:1013–1016.
10.Borisch N, Haussmann P. Radiolunate arthrodesis in the rheumatoid wrist: a retrospective clinical and radiological long-term follow-up. J Hand Surg 2002;27B:61–72.
11.Ishikawa H, Murasawa A, Nakazono K. Long-term follow-up study of radiocarpal arthrodesis for the rheumatoid wrist. J Hand Surg 2005;30A:658–666.
12.Muramatsu K, Ihara K, Tanaka H, Kawai S. Carpal instability in rheumatoid wrists. Rheumatol Int 2004;24:34–36.
13.Besl PJ, Mackay N. A method for registration of 3-D shapes. IEEE Trans Pattern Anal 1992;14:239–256.
14.Goto A, Moritomo H, Murase T, Oka K, Sugamoto K, Arimura T, et al. In vivo three-dimensional wrist motion analysis using magnetic resonance imaging and volume-based registration. J Orthop Res 2005;23:750–756.
15.Oka K, Moritomo H, Murase T, Goto A, Sugamoto K, Yoshikawa H. Patterns of carpal deformity in scaphoid nonunion: a three-dimensional and quantitative analysis. J Hand Surg 2005;30A:1136–1144.
16.Oka K, Doi K, Suzuki K, Murase T, Goto A, Yoshikawa H, et al. In vivo three-dimensional motion analysis of the forearm with radioulnar synostosis treated by the Kanaya procedure. J Orthop Res 2006;24:1028–1035.
17.Moritomo H, Goto A, Sato Y, Sugamoto K, Murase T, Yoshikawa H. The triquetrum-hamate joint: an anatomic and in vivo three-dimensional kinematic study. J Hand Surg 2003;28A:797–805.
18.Moritomo H, Murase T, Goto A, Oka K, Sugamoto K, Yoshikawa H. Capitate-based kinematics of the midcarpal joint during wrist radioulnar deviation: an in vivo three-dimensional motion analysis. J Hand Surg 2004;29A:668–675.
19.Moritomo H, Murase T, Goto A, Oka K, Sugamoto K, Yoshikawa H. In vivo three-dimensional kinematics of the midcarpal joint of the wrist. J Bone Joint Surg 2006;88A: 611–621.
20.Lorensen WE, Cline HE. Marching cubes: a high resolution 3D surface construction algorithm. Computer Graphics 1987;21:163–169.
21.Belsole RJ, Hilbelink DR, Llewellyn JA, Dale M, Ogden JA. Carpal orientation from computed reference axes. J Hand Surg 1991;16A:82–90.
22.Arimitsu S, Murase T, Hashimoto J, Oka K, Sugamoto K, Yoshikawa H, et al. A three-dimensional quantitative analysis of carpal deformity in rheumatoid wrists. J Bone Joint Surg 2007;89B:490–494.
23.Linscheid RL, Dobyns JH, Beckenbaugh RD, Cooney WP, Wood MB. Instability patterns of the wrist. J Hand Surg 1983;8:682–686.
24.Li ZM, Kuxhaus L, Fisk JA, Christophel TH. Coupling between wrist flexion-extension and radial-ulnar deviation. Clin Biomech (Bristol, Avon) 2005;20:177–183.
25.Palmer AK, Werner FW, Murphy D, Glisson R. Functional wrist motion: a biomechanical study. J Hand Surg 1985;10A: 39–46.

Three-Dimensional Corrective Osteotomy of Malunited Fractures of the Upper Extremity with Use of a Computer Simulation System

By Tsuyoshi Murase, MD, PhD, Kunihiro Oka, MD, PhD, Hisao Moritomo, MD, PhD, Akira Goto, MD, PhD, Hideki Yoshikawa, MD, PhD, and Kazuomi Sugamoto, MD, PhD

Investigation performed at the Department of Orthopaedic Surgery, Osaka University Graduate School of Medicine, Suita, Japan

Background: Three-dimensional anatomical correction is desirable for the treatment of a long-bone deformity of the upper extremity. We developed an original system, including a three-dimensional computer simulation program and a custom-made surgical device designed on the basis of simulation, to achieve accurate results. In this study, we investigated the clinical application of this system using a corrective osteotomy of malunited fractures of the upper extremity.

Methods: Twenty-two patients with a long-bone deformity of the upper extremity (four with a cubitus varus deformity, ten with a malunited forearm fracture, and eight with a malunited distal radial fracture) participated in this study. Three-dimensional computer models of the affected and contralateral, normal bones were constructed with use of data from computed tomography, and a deformity correction was simulated. A custom-made osteotomy template was designed and manufactured to reproduce the preoperative simulation during the actual surgery. When we performed the surgery, we placed the template on the bone surface, cut the bone through a slit on the template, and corrected the deformity as preoperatively simulated; this was followed by internal fixation. All patients underwent radiographic and clinical evaluations before surgery and at the time of the most recent follow-up.

Results: A corrective osteotomy was achieved as simulated in all patients. Osseous union occurred in all patients within six months. Regarding cubitus varus deformity, the humerus-elbow-wrist angle and the anterior tilt of the distal part of the humerus were an average of 2° and 28°, respectively, after surgery. Radiographically, the preoperative angular deformities were nearly nonexistent after surgery. All radiographic parameters for malunited distal radial fractures were normalized. The range of forearm rotation in patients with forearm malunion and the range of wrist flexion-extension in patients with a malunited distal radial fracture improved after surgery.

Conclusions: Corrective osteotomy for a malunited fracture of the upper extremity with use of computer simulation and a custom-designed osteotomy template can accurately correct the deformity and improve the clinical outcome.

Level of Evidence: Therapeutic Level IV. See Instructions to Authors for a complete description of levels of evidence.

Treatment of symptomatic osseous deformity of the extremity resulting from a malunited fracture is a challenge. Anatomically accurate correction is the key to obtaining good functional outcomes after corrective osteotomy, especially for the upper extremity[1-4]. However, conventional preoperative planning with two-dimensional plain radiographs has not always provided sufficient information to understand the complex three-dimensional deformity[5-9]. On the other hand, advances in computer technology, such as the development of a multidetector computed tomography scanner and rapid prototyping technology, have made accurate three-dimensional preoperative simulation possible[10-14]. To establish a reliable surgical treatment for malunited extremity fractures, we developed a simulation system consisting of a three-dimensional computer program and a custom-made osteotomy template that allows the reproduction of preoperative simulation during the actual

Disclosure: In support of their research for or preparation of this work, one or more of the authors received, in any one year, outside funding or grants in excess of $10,000 from the Japan Science and Technology Agency and the New Energy and Industrial Technology Development Organization. Neither they nor a member of their immediate families received payments or other benefits or a commitment or agreement to provide such benefits from a commercial entity. No commercial entity paid or directed, or agreed to pay or direct, any benefits to any research fund, foundation, division, center, clinical practice, or other charitable or nonprofit organization with which the authors, or a member of their immediate families, are affiliated or associated.

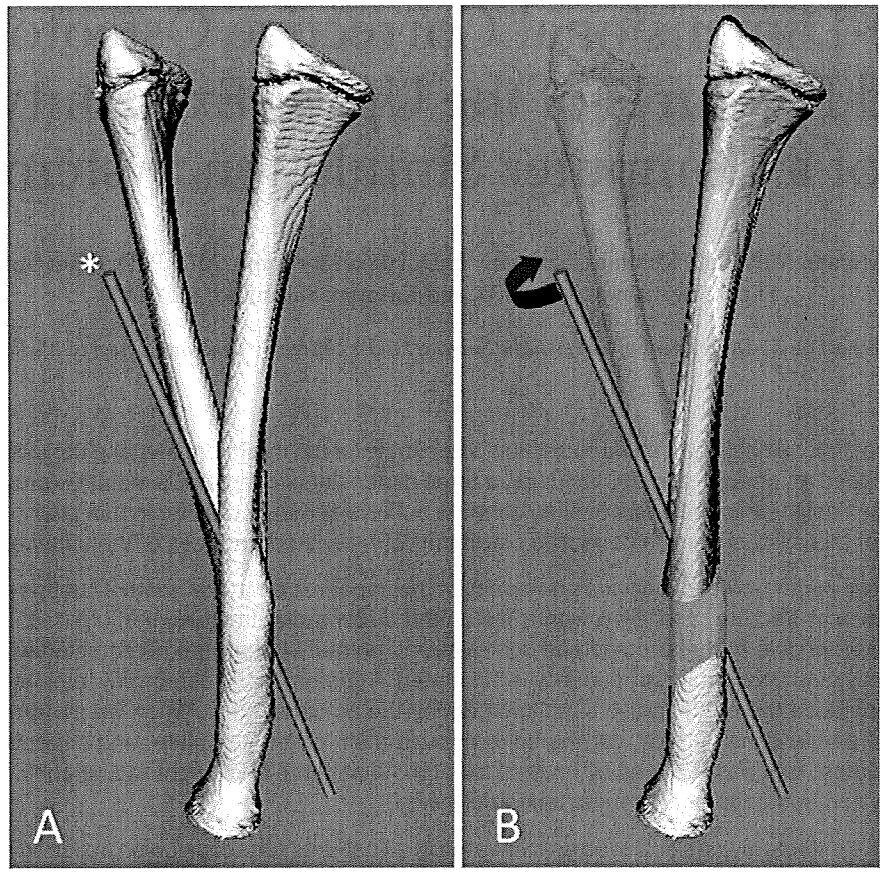

Fig. 1

Malunited radial fracture: By superimposing the malunited radius (yellow) with the mirror image of the contralateral, normal radius (white), we quantified the deformity of the distal part relative to the proximal part, which can be further defined in terms of rotation around and translation along a certain axis using the screw displacement axis technique[21-23]. When the translation is small, it can be simply regarded as the deformity axis (asterisk in A). Correction in this case is to be completed by performing a rotational osteotomy of 45° around the axis on the plane perpendicular to it (curved arrow in B).

surgery[15-17]. This system, despite some shortcomings, such as radiation exposure during computed tomography scanning and the time and expense necessary to develop the custom-made template, is expected to facilitate accurate anatomical correction with a simple osteotomy. The purpose of this study was to investigate the preliminary radiographic and clinical results of corrective osteotomy for malunited fractures of the upper extremity with use of this system.

Materials and Methods

Patients

Between January 2003 and October 2006, twenty-two consecutive patients with twenty-seven malunited fractures of the upper extremities underwent a corrective osteotomy with the use of preoperative simulation and a custom-made osteotomy template. All patients were followed for more than twelve months (range, fourteen to thirty-one months; mean, twenty-two months) (see Appendix). There were fourteen male and eight female patients with a mean age of thirty-two years (range, ten to seventy-two years) at the time of surgery. Our institutional review board approved this study. After informed consent was obtained from patients for participation in the study, a preoperative simulation, corrective osteotomy with use of the custom-made template, and physical and radiographic examinations were carried out.

Inclusion criteria included an osseous deformity of the radius, ulna, or humerus and an age of at least ten years at the time of surgery. Exclusion criteria included malunions of the hand and carpus, deformity with marked shortening that would require gradual lengthening, intra-articular involvement of the adjacent joint, and an age of less than ten years. Deformity of small bones and an age of less than ten years were considered exclusion criteria because the reliability of the operative technique with use of a surgical template for smaller bones had not been established and because active remodeling is expected in younger patients[18].

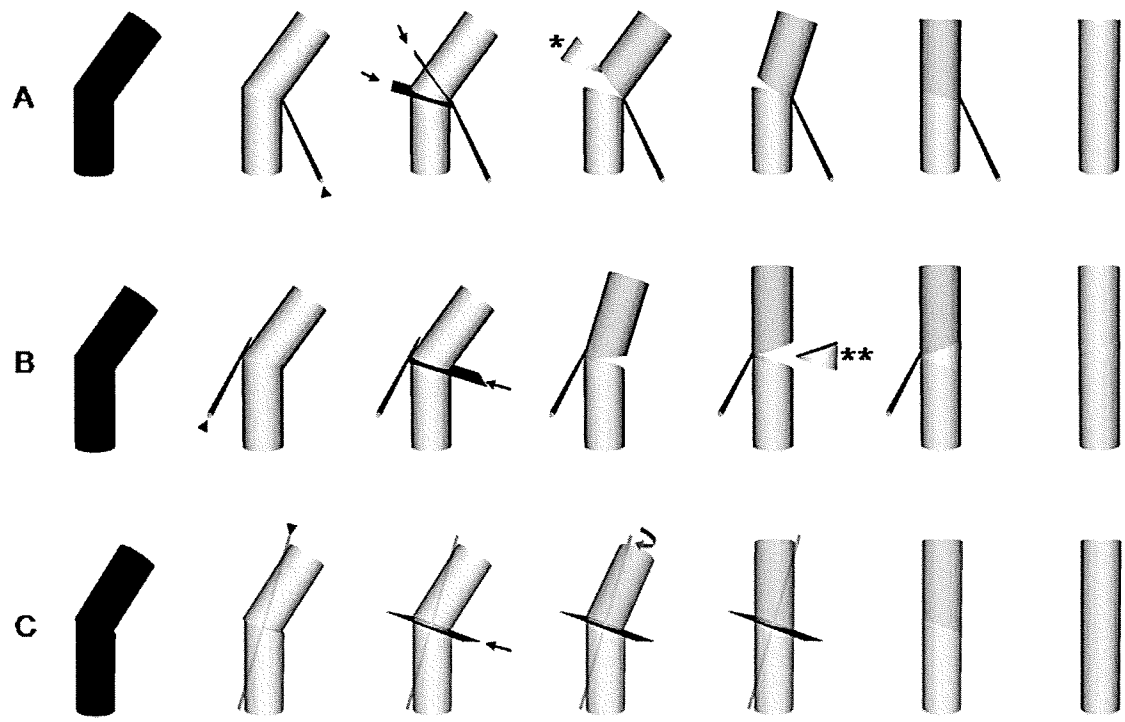

Fig. 2

The bent cylinders represent the deformed bones. Different deformities can show a similar silhouette (the left figures of A, B, and C). The three-dimensional relationship between the bone and the deformity axis (arrowhead of each figure) suggests the most appropriate method of correction. When the axis runs along the concave side of the deformity, a closing osteotomy after removal of a wedge (asterisk) brings about the rotation of the bone segment around the deformity axis, thereby completing the correction (A). When the deformity axis is along the convex side, an opening wedge osteotomy followed by wedge-shaped bone-grafting (double asterisks) is considered appropriate (B). When the axis is nearly parallel to the longitudinal bone axis, a rotational osteotomy (curved arrow) can be conducted in the osteotomy plane, which is perpendicular to the deformity axis (C). If the deformity axis is displaced from the bone, a closing or opening wedge osteotomy with shortening or lengthening is appropriate. The osteotomy planes are indicated by arrows.

This study included four distal humeral malunions (a cubitus varus deformity), ten diaphyseal malunions of the forearm, and eight malunited distal radial fractures. In the ten forearm malunions, the radius was malunited in four, the ulna was malunited in one, and both the radius and the ulna were malunited in five. The average age at the time of injury was 5.6 years for the patients with a cubitus varus deformity, twenty years for those with a forearm malunion, and forty-nine years for those with a malunion of the distal end of the radius. Initial treatment had consisted of closed reduction and cast immobilization in eighteen patients and open reduction and internal fixation in four patients.

At the time of initial presentation to our hospital, all patients demonstrated 5° to 45° of angular deformity of the bone on plain radiographs. Surgery was indicated because of a functional deficit in nineteen patients and an unsightly appearance in three patients. Nine of the ten patients with a forearm malunion had difficulty turning a doorknob and receiving a coin in the open palm because of restricted forearm rotation. The other patient (Case 7), who had malunited fractures of both bones of the forearm, reported recurrent anterior dislocation of the radial head accompanied by pain when he pronated the affected forearm. Three patients with a malunited forearm fracture (Cases 6, 11, and 12) and one patient with a malunited distal radial fracture (Case 20) had distal radioulnar joint subluxation. All of the patients with malunited distal radial fractures reported restricted range of wrist motion, moderate wrist pain, and decreased grip strength, and they experienced difficulty in using the affected hand in daily activities. One patient with cubitus varus (Case 1) could not perform simple activities, such as bringing food to the mouth, with the affected hand because of restricted elbow flexion. The other three patients with cubitus varus complained that the elbow had an unsightly appearance.

Simulation Technique

The affected and the contralateral limbs of all patients were scanned with use of a computed tomography scanner (LightSpeed Ultra 16; General Electric, Waukesha, Wisconsin), at a scan time of 0.5 sec, a scan pitch of 0.562:1, a tube current of 10 to 50 mA, and a tube voltage of 120 kV. Digital data from 0.625-mm slices were sent to a workstation (Precision Work-

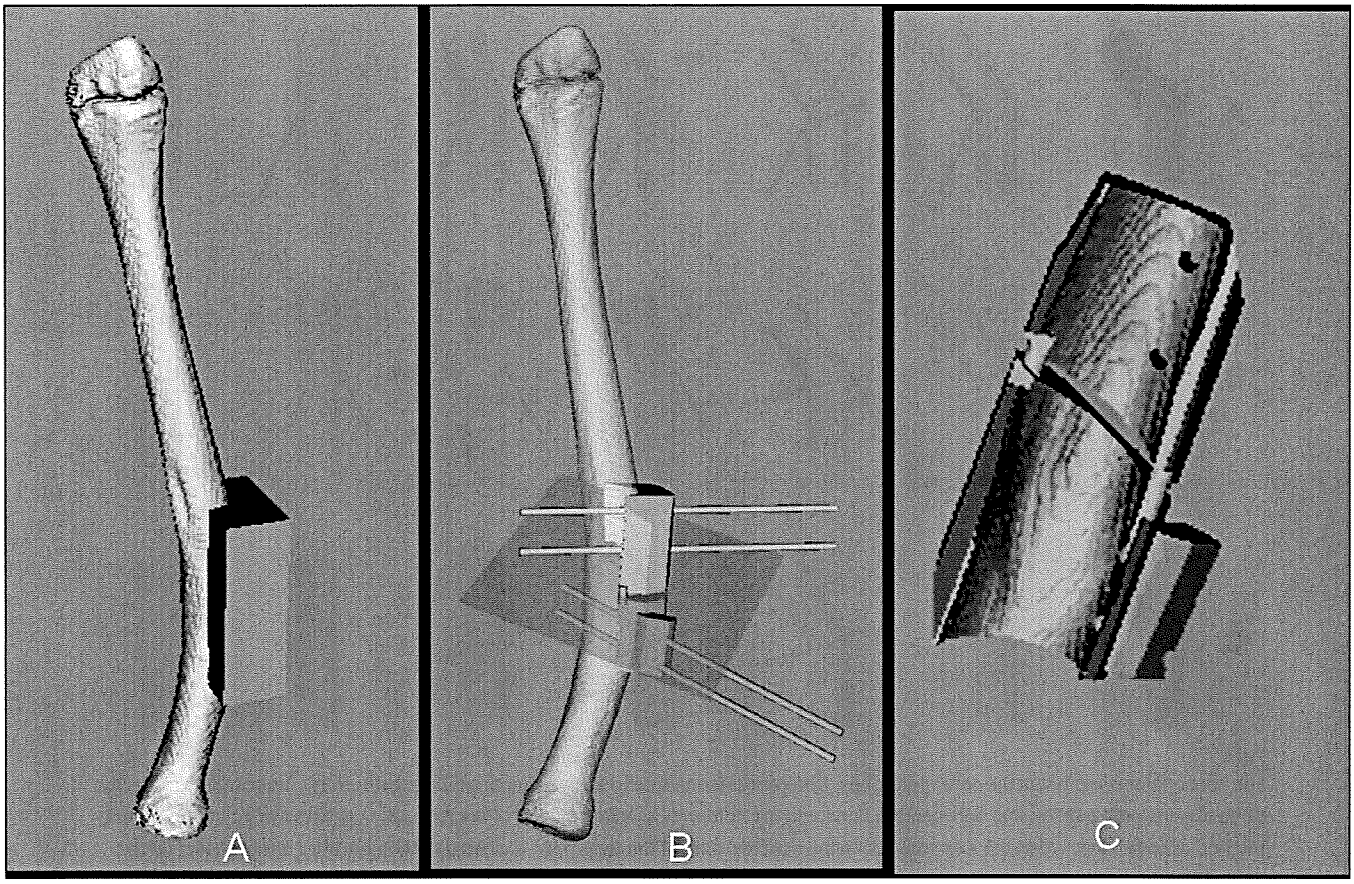

Fig. 3

Fig. 3 On the computer, a block of an appropriate size was placed on the bone surface that was to be exposed during surgery (A). The osteotomy plane, multiple cylinders, and the bone itself were subtracted from the block (B). The cylinders consist of two groups that have an angle of the deformity across the osteotomy plane. Finally, the computer design of the custom-made template was completed by shaping it (C).

Fig. 4 The osteotomy template was embodied as a real plastic model. These figures show the surgeon's side (A) and the bone-contacting side (B) of the template. (Reprinted, with permission, from: Murase T, Moritomo H, Sugamoto K, Yoshikawa H, Ogata K, Kawasaki K. [3D computer simulation for deformity correction of the limb]. Orthop Surg Traumatol. 2005;48:1055-60. Japanese.)

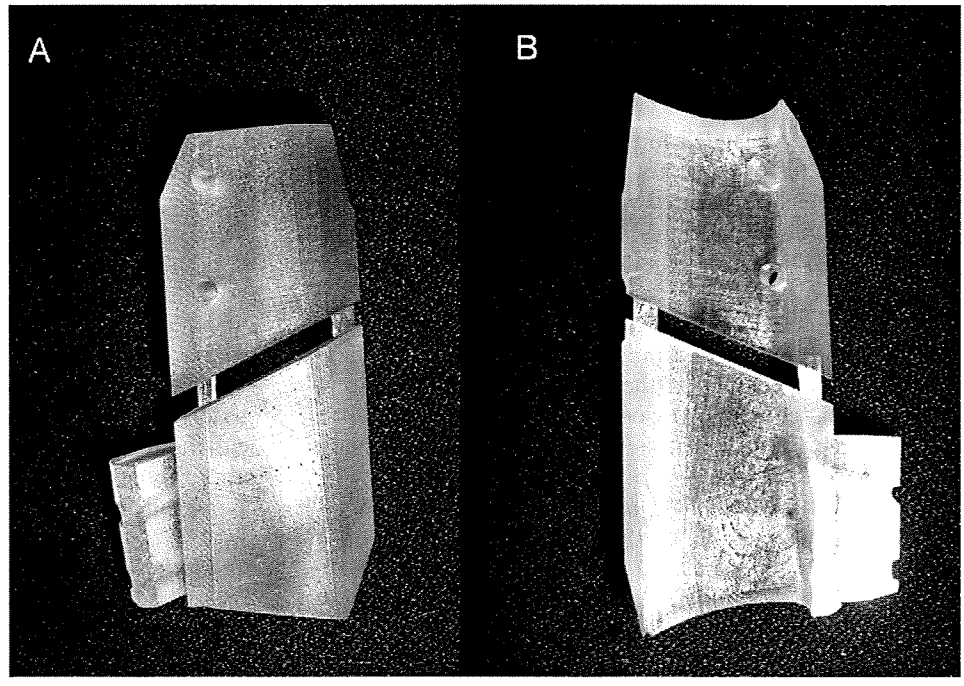

Fig. 4

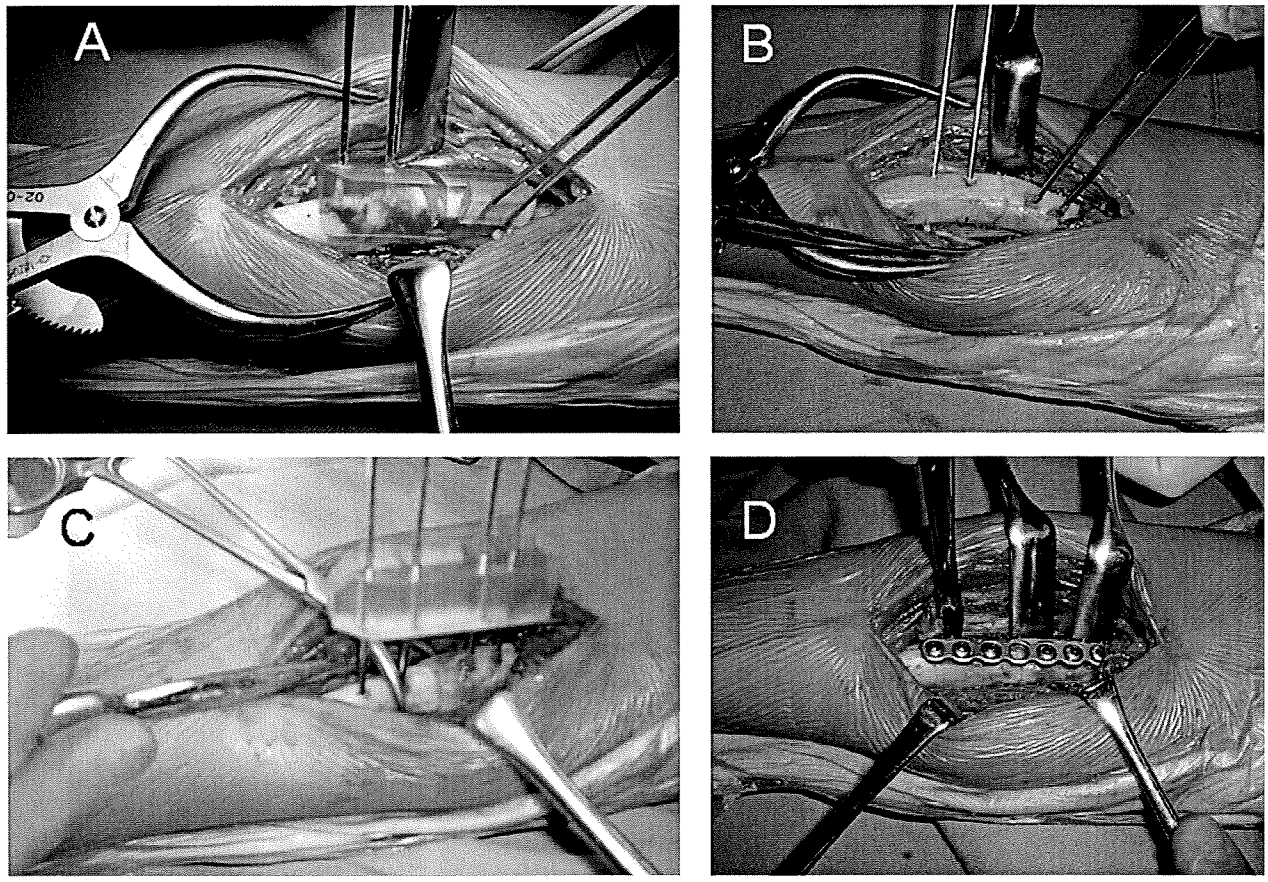

Fig. 5

Case 9. A fourteen-year-old boy with a malunited forearm fracture. The malunited radius was exposed through an anterior approach. The osteotomy template was fitted to the malunited site and fixed with Kirschner wires (A). The bone was divided through the cutting slit in the template, which was then removed (B). A reduction guide was used to maintain the Kirschner wires in a parallel position (C). Internal fixation was then accomplished with a plate and screws (D). (Reprinted, with permission, from: Murase T, Moritomo H, Sugamoto K, Yoshikawa H, Ogata K, Kawasaki K. [3D computer simulation for deformity correction of the limb]. Orthop Surg Traumatol. 2005;48:1055-60. Japanese.)

station 650; Dell, Round Rock, Texas). The malunited bones were segmented, and three-dimensional surface models were constructed by applying three-dimensional surface generation of the cortex of the bone[19] with use of the original computer program based on the Visualization Toolkit (Kitware, Clifton Park, New York). On the computer, the deformity of the affected bone was evaluated by superimposing[20] it with the goal model (e.g., the mirror image of a contralateral, normal bone), which can be further determined in terms of rotation around and translation along one unique axis, i.e., the three-dimensional deformity axis, with use of the screw displacement axis technique[21-23] (Fig. 1, *A*) (see Appendix for Videos 1 and 2). On the basis of the information obtained about the deformity axis, a corrective osteotomy was simulated[24,25] (Figs. 1, *B* and 2).

Design and Manufacturing of the Custom-Made Osteotomy Template

To reproduce the preoperative simulation during the actual surgery, we developed an operative method using a custom-made osteotomy template that was designed on the basis of a preoperative three-dimensional computer simulation with use of commercially available software (Magics RP; Materialise, Leuven, Belgium) and was embodied as a plastic model through rapid prototyping technology (Eden250; Objet Geometries, Rehovot, Israel, or Viper si2; 3D Systems, Rock Hill, South Carolina) with medical grade resin (Figs. 3 and 4). The custom-made osteotomy template has a shape that closely fits the bone surface and an osteotomy slit or slits and drill-holes that guide the insertion of the Kirschner wires. The slit guides the precise osteotomy cut; and the two sets of Kirschner wires, inserted through the drill-holes at an angle of the deformity, indicate that the reduction is completed when they become parallel to each other. A reduction guide to maintain the parallel position of the Kirschner wires is prepared preoperatively in the same manner as is the custom-made osteotomy template (see Appendix for Video 3).

Surgical Technique

During the procedure, the template was placed on the bone surface, the bone was osteotomized through a slit in the tem-

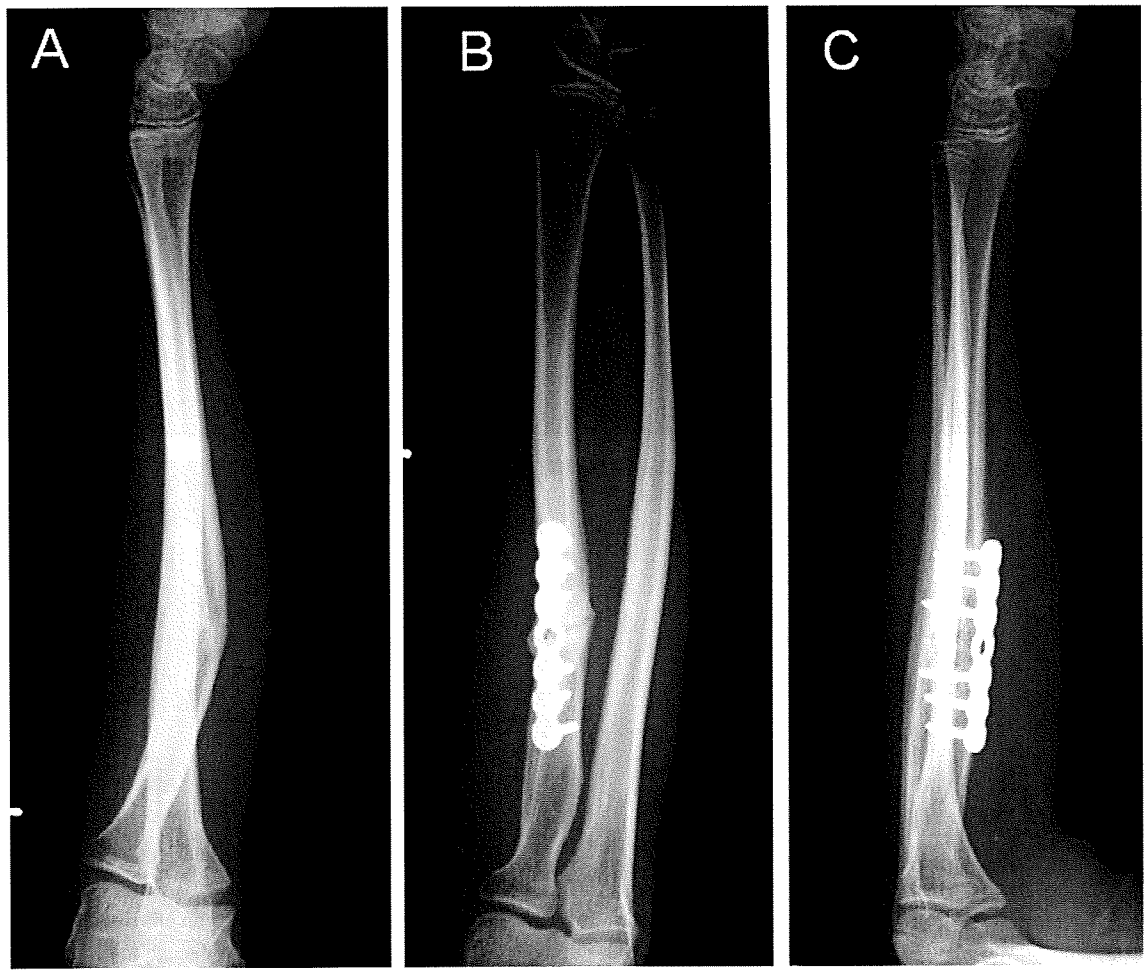

Fig. 6

Case 9. The preoperative anteroposterior radiograph of the forearm (A) shows anterior bowing of the radius. The postoperative anteroposterior (B) and lateral (C) radiographs show good anatomical correction. Note that the forearm is in a semipronated position preoperatively because of restricted forearm supination and is in a supinated position postoperatively. (Reprinted, with permission, from: Murase T, Moritomo H, Sugamoto K, Yoshikawa H, Ogata K, Kawasaki K. [3D computer simulation for deformity correction of the limb]. Orthop Surg Traumatol. 2005;48:1055-60. Japanese.)

plate, and the deformity was corrected as simulated preoperatively (Figs. 5 and 6). We were able to perform all osteotomies as preoperatively simulated. This was followed by internal fixation (plates and screws were used in twenty-four bones; Kirschner wires, including tension band wiring, were placed in two bones; and both methods of fixation were used in one bone). The template was fitted to the bone surface with reference to the characteristic configuration of the malunion and anatomical landmarks (e.g., the Lister tubercle, humeral condyles, and olecranon fossa). In patients with a malunited forearm fracture, the distance between the osteotomy site and the radial or ulnar styloid was calculated preoperatively on the computer and also served as a reference. A rotational osteotomy was performed on ten bones, a closing wedge osteotomy was done on five bones, and an opening wedge osteotomy with bone graft was performed on twelve bones. The amount of correction, which was the rotation around the three-dimensional deformity axis, ranged from 13° to 67°, with an average of 32°. In two rotational osteotomies, 3-mm and 2-mm shortenings along the deformity axis were required. In the other three rotational osteotomies, 2, 10, and 4-mm lengthenings with an interposition bone graft were required. These shortenings and lengthenings were performed to correct radioulnar discrepancies. The osteotomy template and the reduction guide were designed with consideration of these longitudinal adjustments. Open reduction of distal radioulnar joint subluxation in three patients with malunited forearm fractures (Cases 6, 11, and 12) and osteosynthesis of an ulnar styloid nonunion in one patient with a malunited distal radial fracture (Case 21) were combined with the corrective osteotomy.

The average time between the initial injury and the corrective osteotomy was thirteen years (range, two to twenty-seven years) for cubitus varus deformity, thirty months (range, six to 100 months) for malunited forearm fractures, and twelve

TABLE I Results of Corrective Osteotomy for Cubitus Varus Deformity

	Radiographic Evaluation							Clinical Evaluation*			
		Humerus-Elbow-Wrist Angle† *(deg)*			Tilting Angle† *(deg)*			Range of Elbow Flexion-Extension *(deg)*		Pain	
Case	Time to Bone Union *(mo)*	Preop.	Postop.	Normal Side	Preop.	Postop.	Normal Side	Preop.	Postop.	Preop.	Postop.
1	2	−15	5	5	−10	25	25	95/35	130/10	None	None
2	5	−20	5	6	30	32	35	140/5	140/0	None	None
3	3	−23	4	7	27	25	25	130/−25	130/−20	None	None
4	3	−21	−5	7	30	30	30	140/−10	135/−5	None	None
Avg.	3.3	−19.8	2.3	6.3	19.3	28.0	28.8	126/1	134/−4		

*No significant difference was found between preoperative and postoperative ranges of elbow motion and pain. †No significant difference was found between the postoperative radiographic parameters and those of the unaffected, normal side. Negative values for the humerus-elbow-wrist angle and the tilting angle represent varus and hyperextension deformity of the distal part of the humerus, respectively.

months (range, five to twenty-three months) for malunited distal radial fractures.

Radiographic and Clinical Evaluation

Radiographic and clinical evaluations were conducted for all patients before surgery and at the most recent follow-up evaluation. Union was considered complete when the osteotomy line had disappeared and osseous trabecular continuity was confirmed. For cubitus varus deformities, the humerus-elbow-wrist angle[26] (defined by the longitudinal humeral axis and a line passing through the proximal and distal midpoints of the radius and ulna) and the tilting angle[27,28] (the anterior tilt of the articular condyles with respect to the long axis of the humerus) were examined with anteroposterior and lateral radiographs of the upper extremity made with the forearm in a supinated position. For malunited forearm fractures, anteroposterior and lateral radiographs made with the forearm in neutral position or in full supination were compared with

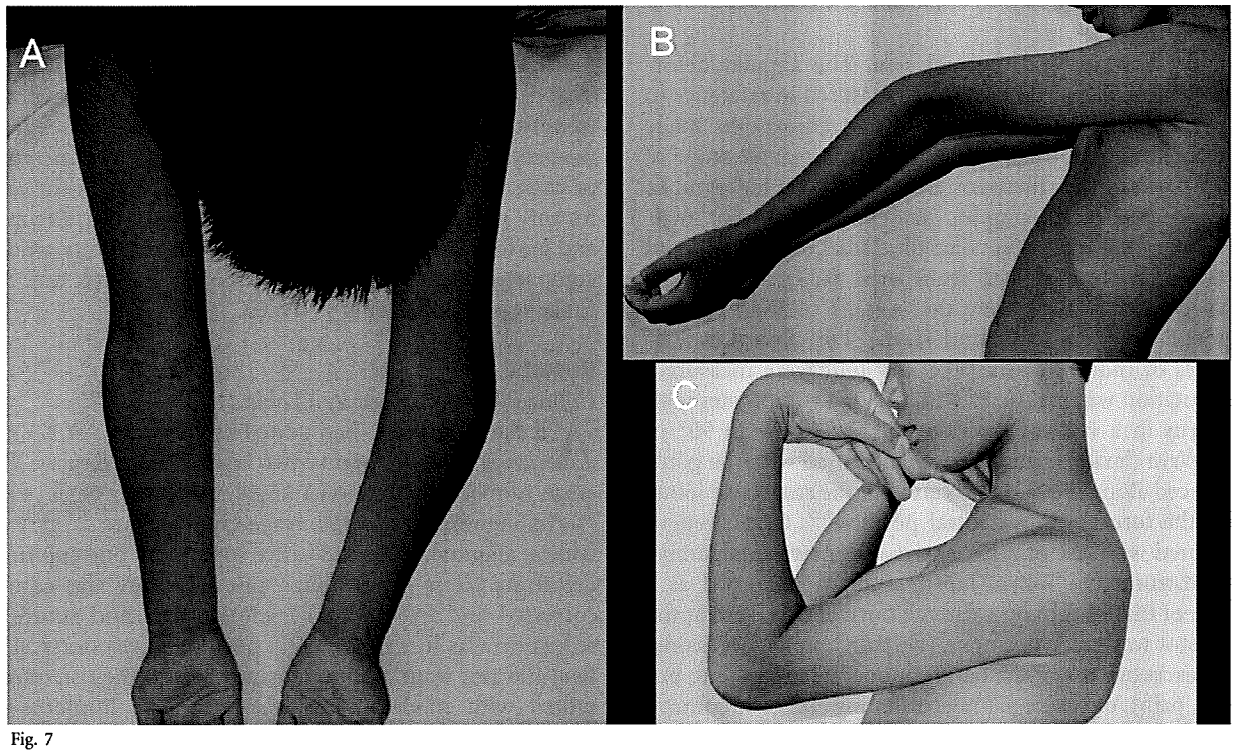

Fig. 7

Case 1. A ten-year-old boy presented with a left cubitus varus deformity (A) accompanied by hyperextension of the elbow (B) and restriction of elbow flexion to 95°(C).

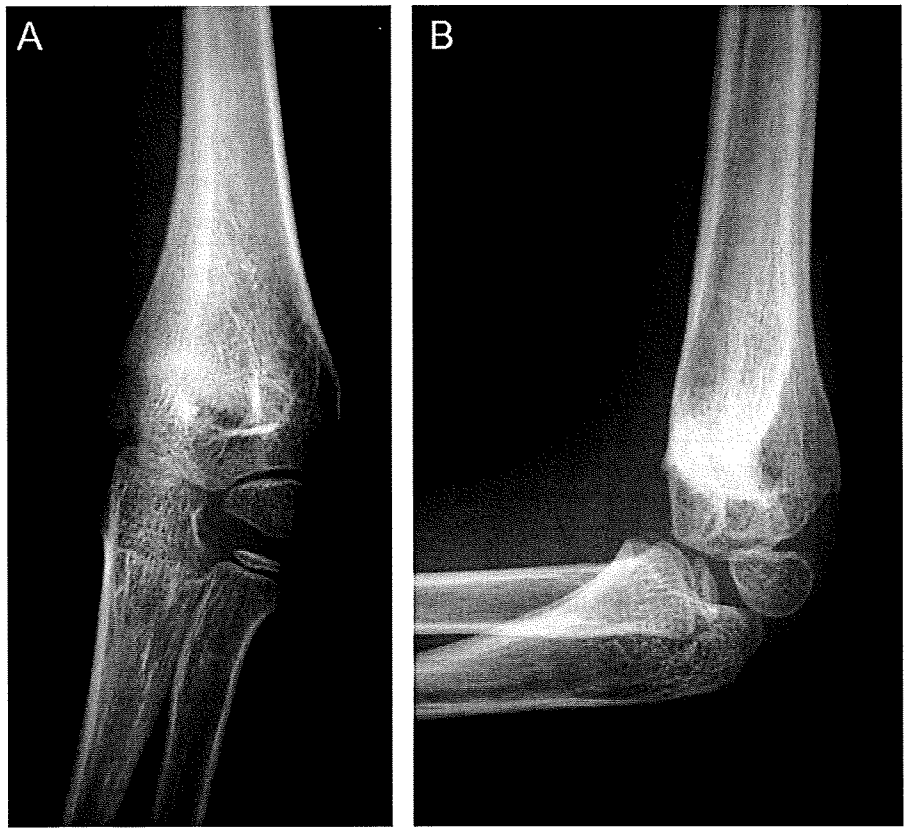

Fig. 8

Case 1. Preoperative anteroposterior (A) and lateral (B) radiographs show the varus and hyperextension deformity of the distal end of the humerus.

those of the contralateral, normal side. The angular deformities of the radius and/or ulna were measured in reference to the contralateral forearm with use of the radiographs made with the forearm in the same position[29]. The greater angle of deformity between the anteroposterior and lateral radiographs was defined as the radiographic deformity angle. For malunited distal radial fractures, volar tilt, radial inclination, and ulnar variance were evaluated from wrist radiographs[30]. The values used in our study were the average of those of two independent reviewers (K.O. and H.M.). For clinical evaluation, ranges of motion of the adjacent joint were measured. Forearm rotation was measured with use of a goniometer with the humerus in a vertical position and the elbow in 90° of flexion[31]. Wrist flexion-extension was measured with the goniometer placed along the axis of rotation of the respective joints and with the forearm in a neutral position[9,32]. Grip strength was measured with use of a Jamar dynamometer (Matsumiya Medical Instruments, Tokyo, Japan) and was recorded as a percentage of that of the contralateral, normal side. Pain at the adjacent joint was graded as none (no pain), mild (occasional pain with excessive use of the hand), moderate (persistent, but endurable, pain), or severe pain necessitating analgesic control. The level of satisfaction was graded by the patient as very satisfied, satisfied, neither satisfied nor dissatisfied, dissatisfied, or very dissatisfied[33].

Statistical Methods

The differences between the radiographic values of the extremity that had been operated upon and the values from the normal side, and the differences between the preoperative and postoperative range of motion and grip strength for each deformity group, were determined by paired t test. Preoperative and postoperative scores for pain in each deformity group were compared with use of the Wilcoxon signed-rank test. Significance was established at $p < 0.05$.

Results

Cubitus Varus Deformity (Table I)

All osteotomy sites had united by an average of 3.3 months (range, nine to twenty-two weeks) after surgery. The average humerus-elbow-wrist angle and tilting angle were 20° (varus alignment) and 19°, respectively, before surgery and 2° (valgus alignment) and 28° after surgery. In one cubitus varus deformity (Case 4), although the deformity was completely corrected and fixed with Kirschner wires and suture wires, reduction was lost in the early postoperative course. The patient did not want additional surgery, and the osteotomy site united with moderate displacement. The humerus-elbow-wrist angle in this patient had been 21° (varus alignment) before surgery, 7° (valgus alignment) just after surgery, and 5° (varus alignment) at the most recent follow-up evaluation.

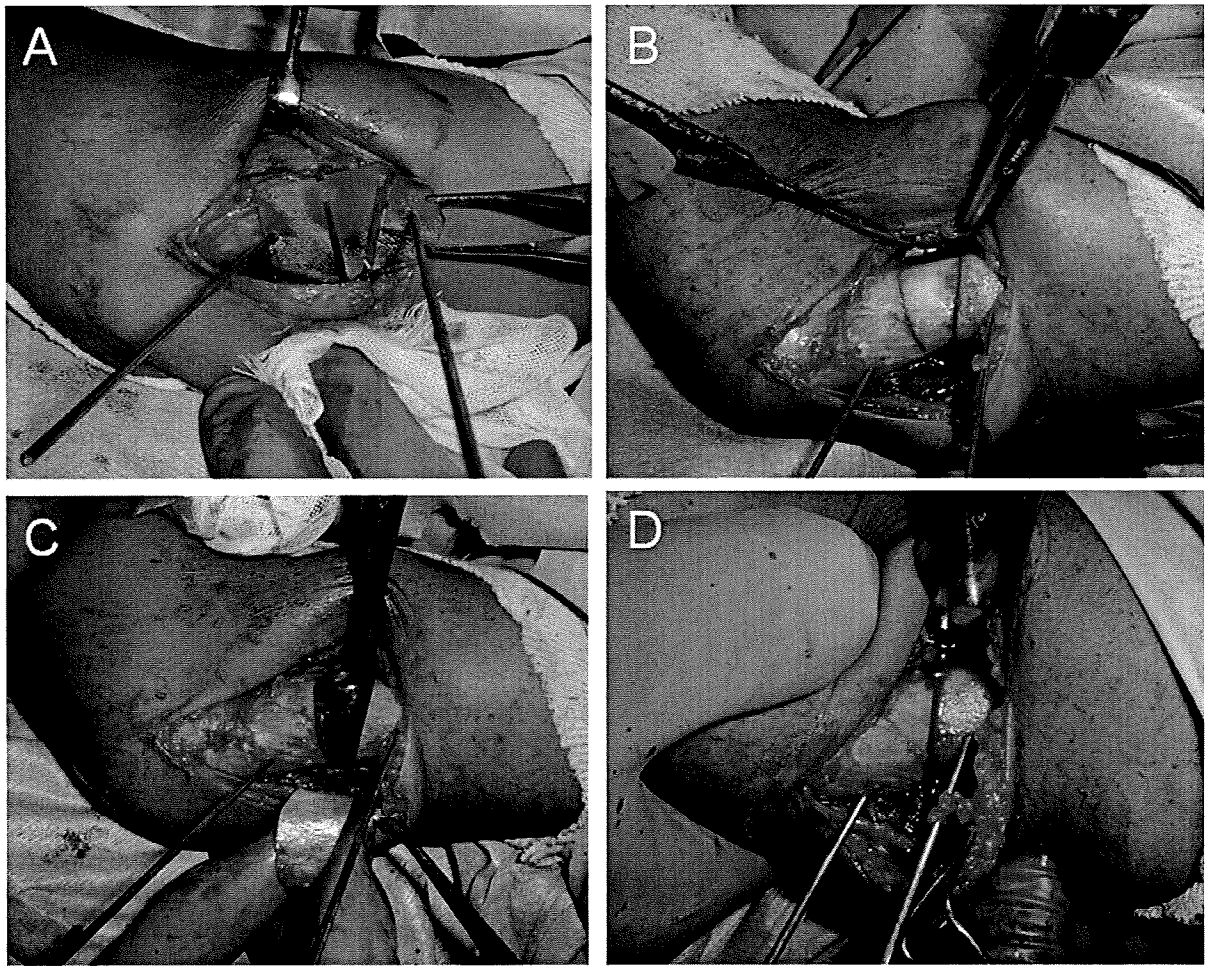

Fig. 9

The osteotomy template has been placed on the dorsolateral surface of the humerus through a lateral approach and fixed with Kirschner wires (A). The osteotomy has been accomplished through the slits on the template, which was then removed (B and C), and the osteotomy site was closed (D).

Except for this patient, the average humerus-elbow-wrist angle improved from 19° (varus alignment) before surgery to 5° (valgus alignment) after surgery. One patient with a cubitus varus deformity (Case 1) who had elbow hyperextension and restricted flexion attained normal range of elbow motion after surgery (Figs. 7 through 11). The range of elbow joint motion of the other patients with cubitus varus did not change significantly. Three patients were very satisfied with the operation, and one patient (Case 4) was neither satisfied nor dissatisfied with the operation. One patient (Case 2) complained of mild discomfort around the hardware, which was subsequently removed.

Malunited Forearm Fracture (Table II)

The osteotomy sites united an average of sixteen weeks (range, eight to twenty-six weeks) after surgery. The average angle of deformity before surgery was 16° (range, 5° to 33°) compared with the normal side. It was well corrected to 1° (range, 0° to 3°) after surgery. No distal radioulnar joint discrepancy was observed on the radiographs of the involved forearm compared with the normal side. The average range of forearm pronation and supination significantly improved from 60° and 19°, respectively, before the operation to 82° and 73° after the operation ($p < 0.01$ for both). Restricted forearm supination persisted in one patient (Case 5) with malunited fractures of both bones of the forearm, although the malunions were well corrected. In this patient, the initial injury had occurred when the patient was seven years old, and corrective surgery was performed when she was sixteen years old. It was believed that changes in joint configurations and soft-tissue contractures during this long period of time were the cause of the residual restricted forearm supination. Five patients reported pain in the adjacent joint before surgery; four of them (Cases 6, 11, 12, and 14) experienced pain in the distal radioulnar joint and one (Case 7) had pain in the proximal radioulnar joint. The preoperative pain experienced by all of these patients disappeared or decreased substantially after surgery. Painful recurrent dislocation of the radial head in one patient (Case 7), with mal-

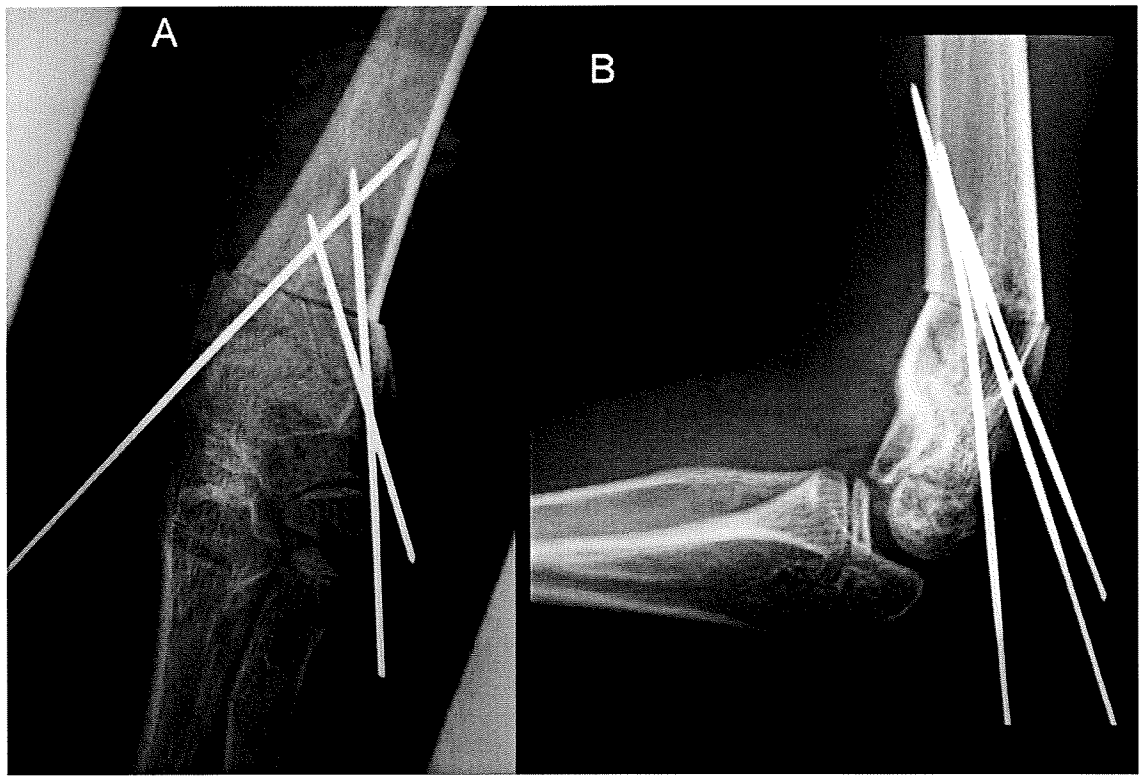

Fig. 10

Appropriate correction was obtained as evident on the anteroposterior (A) and lateral (B) radiographs made after the closing wedge osteotomy.

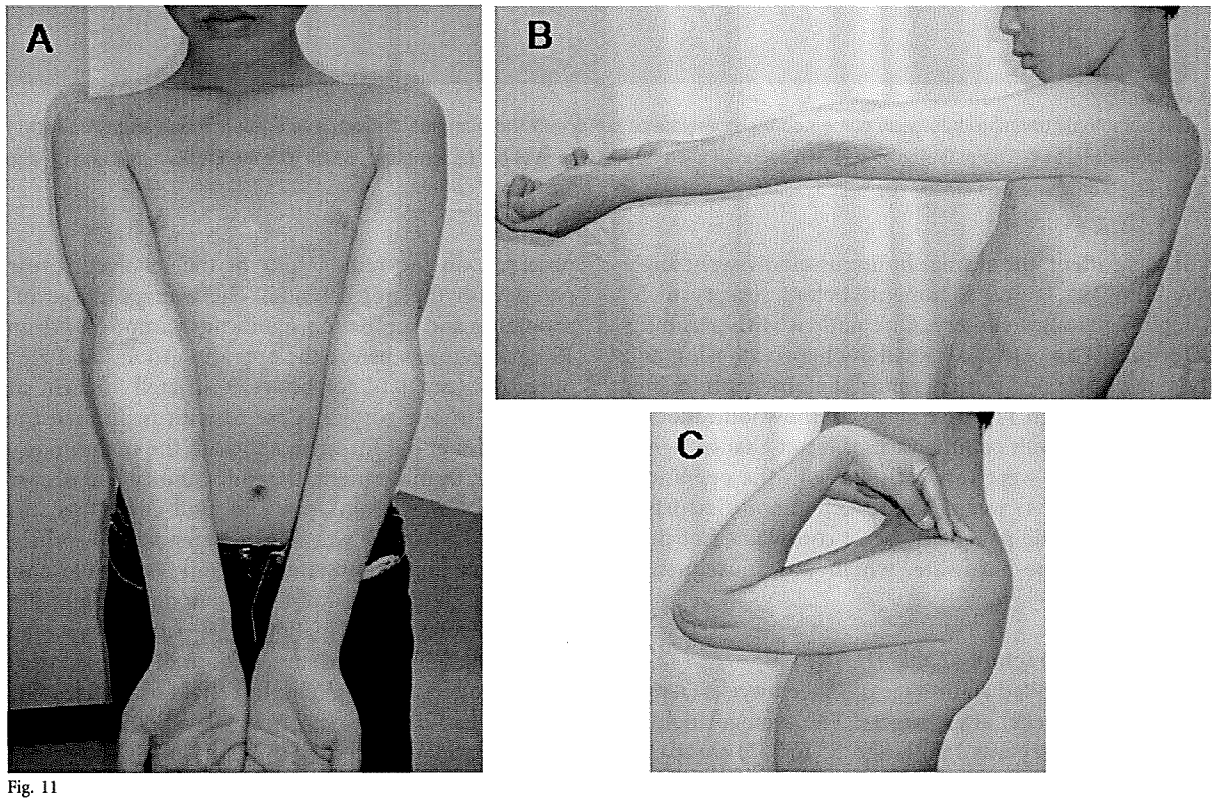

Fig. 11

The varus deformity has been corrected (A), and hyperextension and flexion of the elbow improved after surgery (B and C).

TABLE II Results of Corrective Osteotomy for Malunited Forearm Fractures

	Radiographic Evaluation				Clinical Evaluation				
			Deformity Angle* *(deg)*		Range of Forearm† (Pronation/Supination) *(deg)*			Pain†	
Case	Malunited Bone	Time to Bone Union *(mo)*	Preop.	Postop.	Preop.	Postop.	Normal Side	Preop.	Postop.
5	Radius	6	12	0	80/−30	80/10	80/90	None	None
	Ulna	6	5	0					
6	Radius	4	10	3	50/45	60/70	90/90	Moderate	Mild
	Ulna	4	5	0					
7	Radius	3	18	0	90/90	90/90	90/90	Moderate	None
	Ulna	4	16	2					
8	Radius	5	33	0	10/15	95/80	80/95	None	None
	Ulna	4	15	3					
9	Radius	3	22	0	60/−20	70/70	80/90	None	None
10	Radius	3	25	0	80/30	90/90	90/90	None	None
11	Radius	4	15	0	90/0	85/75	85/90	Mild	None
12	Radius	3	21	2	50/−15	80/70	90/70	Moderate	Mild
13	Ulna	2	30	0	10/60	80/90	80/90	None	None
14	Radius	4	6	0	80/10	90/80	90/90	Moderate	None
	Ulna	3	13	0					
Avg.		3.8	16.4	0.7	60/19	82/73	86/89		

*The deformity angle was the angle of radiographic angular deformity measured in reference to the contralateral, normal bone in the same position (see Radiographic and Clinical Evaluation section). †A significant difference was found between the preoperative and postoperative values ($p < 0.01$). ‡No significant difference was found between the preoperative and postoperative level of pain.

united fractures of both bones of the forearm, disappeared after corrective osteotomy without soft-tissue reconstruction, and the patient was able to resume sports activity. Six patients were very satisfied, and four patients were satisfied with the surgery.

Malunited Distal Radial Fracture (Table III)

All osteotomy sites had united an average of ten weeks (range, eight to thirteen weeks) after surgery. The mean volar tilt, radial inclination, and ulnar variance were −17°, 14°, and 3.4 mm, respectively, before the operation and 8°, 23°, and 0.6 mm at the final follow-up evaluation. The average wrist flexion and extension improved from 33° and 54°, respectively, before surgery to 62° and 66° after surgery ($p < 0.01$ for both). The average ranges of forearm pronation and supination improved from 58° and 69°, respectively, before surgery to 79° and 78° after surgery ($p = 0.042$). Restricted forearm supination persisted in one patient (Case 20), although the malunion was well corrected. In this patient, we believe that preexisting distal radioulnar subluxation that was not addressed well during surgery was the cause of the residual forearm rotation loss. The average grip strength improved from 42% to 86% of that of the normal side. All eight patients experienced wrist pain before surgery, which disappeared or decreased after surgery ($p = 0.013$). Three patients (Cases 16, 21, and 22) complained of discomfort around the hardware, which was subsequently removed. Four patients were very satisfied, three were satisfied, and the remaining patient (Case 20) was neither satisfied nor dissatisfied with the operation.

Complications

Postoperative partial loss of correction occurred in one patient with cubitus varus deformity. One patient who underwent surgery for cubitus varus deformity and three patients who underwent surgery for a malunited distal radial fracture complained of hardware-related pain or discomfort that necessitated hardware removal. Distal radioulnar subluxation in one patient with a malunited distal radial fracture persisted after surgery. No other major complications, including nonunion, neurovascular compromise, or infection, were observed.

Discussion

Malunion of the forearm bones, cubitus varus deformity, and a malunited distal radial fracture are typical posttraumatic deformities of the upper extremity. Symptoms and functional impairments related to these deformities may cause serious disabilities[26,30,31,34-36]. Although corrective osteotomies have been performed to improve the function and appearance

TABLE III Results of Corrective Osteotomy for Malunited Distal Radial Fractures

	Radiographic Evaluation								
		Volar Tilt*† *(deg)*			Radial Inclination* *(deg)*			Ulnar Variance* *(mm)*	
Case	Time to Bone Union *(mo)*	Preop.	Postop.	Normal Side	Preop.	Postop.	Normal Side	Preop.	Postop.	Normal Side
15	3	−20	10	10	13	25	26	4	2	1.5
16	2	−10	9	10	−2	20	23	2	0	0
17	2	−25	5	7	15	27	28	3	0	0
18	2	−22	5	5	20	23	24	3	1.5	1
19	2	−10	5	5	10	22	23	3	0	0
20	3	−15	8	7	16	25	24	2	0	0
21	3	0	8	8	21	23	23	3	1	0
22	2	−35	10	10	15	19	20	7	0	0
Avg.	2.4	17	8	8	14	23	24	3.4	0.6	0.3

*No significant difference was found between the postoperative radiographic parameters and those of the unaffected, normal side. †A negative value for volar tilt represents extension of the articular surface. ‡A significant difference was found between the preoperative and postoperative values ($p < 0.05$). §A significant difference was found between the preoperative and postoperative values ($p < 0.01$).

of the extremity, it is not easy to correct three-dimensionally complex osseous deformities accurately[2-4,7,8,16,31,37]. Previous studies have suggested the usefulness of frontal and sagittal radiographs in the preoperative planning of a corrective osteotomy, although estimation of three-dimensional deformities with two-dimensional images has limitations[5,6,9,12,38,39]. Failure to make an accurate correction may lead to inferior clinical results, especially in the upper extremity, where anatomical bone configuration is of considerable importance to function[3-5,8,9,31,35,38,39]. To solve these problems, we developed a novel computer-assisted system to guide corrective osteotomy[15-17]. Our program can indicate the optimum pattern and plane of corrective osteotomy by calculating the axis and amount of three-dimensional deformity. The osteotomy template navigates the surgical procedure to realize the preoperative simulation.

Restricted forearm rotation is the key problem associated with malunions of the forearm bones[4,35,36,39]. Correct rotational alignment, restoration of normal length, and achievement of axial alignment of both bones are necessary to obtain a good range of forearm rotation[40]. Cadaver and clinical studies have suggested that angular deformity of the radius and/or ulna of >10° causes limitations of forearm rotation[3,4,31,39], although the relation between the severity of the deformity and the decrease in forearm rotation has not been clearly established. Contracture of the interosseous membrane, the distal and proximal radioulnar joint capsules, and other surrounding soft tissues is an additional cause of restricted forearm rotation. In long-standing forearm deformity, a combination of these factors is probably responsible for the substantial pathology of restricted range of forearm rotation[36]. In corrective surgery, the challenge is to reduce two parallel rotating long bones while maintaining the congruity of the adjacent joints[35]. Trousdale and Linscheid[36] reported the clinical results of corrective osteotomy of forearm malunion. The average arc of forearm rotation improved to only 102° in chronic forearm malunions treated more than twelve months after the initial injury, whereas it improved to 156° in those treated within twelve months of the initial injury. They concluded that corrective osteotomy for a posttraumatic malunion was best performed within twelve months of the initial fracture. They did not refer to any radiographic parameters. In our series, the average forearm rotation in the patients managed late and in those managed early improved to 152° and 159°, respectively, and angular deformities were well corrected in both groups. Although restricted forearm supination remained in one patient (Case 5), who had undergone surgery nine years after the initial injury, the range of forearm rotation had improved by 40° at the time of the final follow-up. These results indicate that an accurate three-dimensional correction of a deformity of the forearm bones can yield reasonable improvement in forearm motion, even when performed long after the initial injury.

Cubitus varus deformity is a malunion of the distal end of the humerus that generally includes varus, internal rotation, and hyperextension deformities[8,9,28,41]. In the past, it was considered a cosmetic problem, and correction of varus deformity alone has been an accepted practice[26,42,43]. Recently, because joint laxity[34,44] and tardy ulnar nerve palsy[45,46] have been reported as late complications, several investigators have advocated that correction of frontal plate angular deformity is not enough and that rotational deformity should also be corrected[8,9,41]. In fact, internal rotation of the distal end of the humerus of >25° exists in 22% of patients with a cubitus varus deformity[47]. In our opinion, this should not be overlooked,

TABLE III (*continued*)

Clinical Evaluation									
Range of Forearm Motion† (Pronation/Supination) *(deg)*			Range of Wrist Motion§ (Flexion/Extension) *(deg)*			Grip Strength§ *(% of Normal Side)*		Pain†	
Preop.	Postop.	Normal Side	Preop.	Postop.	Normal Side	Preop.	Postop.	Preop.	Postop.
60/90	80/90	80/90	30/55	70/75	80/70	13	83	Moderate	None
60/45	90/90	90/90	30/35	60/70	70/70	22	82	Moderate	Mild
60/90	75/80	90/90	20/60	65/65	70/70	75	95	Moderate	None
10/90	90/90	90/90	25/70	70/70	70/70	48	95	Moderate	None
65/70	90/90	90/90	40/65	70/85	75/85	50	97	Moderate	None
80/10	70/10	90/90	50/30	40/20	70/70	–	–	Mild	Mild
60/80	60/90	90/90	50/60	50/65	70/70	63	75	Moderate	None
70/80	80/80	80/80	20/60	75/80	80/80	26	76	Moderate	None
58/69	79/78	88/89	33/54	62/66	73/73	42	86		

considering its effect on shoulder motion and the appearance of the extremity[48]. Previously reported attempts at three-dimensional correction, however, were based on preoperative planning with use of data from plain radiographs and changes in the range of shoulder motion[9,28,43]. This procedure was also criticized for its technical difficulty and the poor osseous contact achieved at the osteotomy site[26]. In contrast, our system provides a simple and accurate correction based on three-dimensional data. The contact area at the osteotomy site can be visualized easily with use of three-dimensional images, which allow practical planning. The results of the present study, in which the postoperative humerus-elbow-wrist angle was an average of 5° and was within 3° of that of the contralateral, normal side, were the same as or better than those of previous studies[8,41,42]. Yamamoto et al.[28] performed a three-dimensional corrective osteotomy in seven patients, and a hyperextension deformity ranging from 5° to 20° persisted after surgery in three patients. In our series, the tilting angle improved to 28°, on the average, and was almost the same as that of the contralateral, normal side in all patients, including one patient (Case 1) who had 35° of hyperextension deformity before surgery.

Malunion of the distal end of the radius is one of the most common deformities of the upper extremity. Dorsal tilt, radial shortening, and a decrease in radial inclination have been cited by several investigators when attempting to plan three-dimensional correction with use of plain radiographs[1,2,49-53]. Fernandez[49,50] suggested preoperative planning with use of frontal and sagittal plane radiographs and reported good clinical results, with postoperative ranges of 50° of flexion and 57° of extension at the wrist at the time of the final follow-up. However, dorsal tilt of the distal end of the radius remained in eight of the thirty-five patients, and radial shortening of >2 mm persisted in four of the thirty patients, in whom ulnar head resection was not performed. Athwal et al.[38] introduced a computed tomography-based computer-assisted three-dimensional surgical planner that calculates the corrected position of the distal end of the radius, including an evaluation of rotational deformity with use of the contralateral, normal wrist as the template. They applied an intraoperative guidance system, which linked the preoperative plan to an optical tracking device. In six patients, the radiographic parameters of radial inclination, volar tilt, and ulnar variance relative to the contralateral, normal wrist were 2°, 1°, and 0.4 mm, respectively. At the time of the final follow-up, the average ranges in wrist flexion and extension were 47° and 42°, respectively. However, an optical tracking system requires bulky equipment and computers, monitors, and a system operator to be present during the surgery. In our series, the error between the preoperative simulation and postoperative result was <1° for both radial inclination and volar tilt and 0.3 mm for ulnar variance. As for wrist range of motion, the average ranges of wrist flexion and extension at the time of the final follow-up were 62° and 66°, respectively. The radiographic and clinical results of correction for malunited distal radial fractures in the present study were comparable or superior to those of previous studies, and the small custom-made template was quite practical. We could exactly adjust the postoperative ulnar variance in computer simulation and could avoid ulnar head resection, which has often been performed with conventional osteotomies[49,50,54].

The preliminary results in our twenty-two patients indicate that this simulation technique is a clinically reliable method. Three-dimensionally complex deformities can be accurately corrected with a simple one or two-plane osteotomy. The shortcomings of our technique include radiation exposure during computed tomography scanning, the time and effort required for computer simulation, the cost of the custom-made template, and the use of software that is not available to the public. A previous experimental study showed that radiation exposure with this system can be reasonably reduced compared with typical doses of radiation from conventional

diagnostic computed tomography scanning[55]. Computer simulation takes two to three hours for a trained operator. The time and cost of manufacturing the template are three to eight hours and about US$50, respectively. The software is currently used only in our institute for this specific clinical study; however, we plan to distribute it in the near future.

Because this study is based on a preliminary series, it has several limitations such as a relatively small number of patients in each of the corrective osteotomy groups and the absence of a control group. An additional criticism is that a minor deformity after a distal radial fracture could be corrected reasonably well without use of this technique. Therefore, further investigation is needed to determine its clinical value. However, the results of this series are encouraging. We hope that the three-dimensionally accurate correction realized by our technology will contribute to the field of deformity correction of the upper extremities.

Appendix

eA A table showing the clinical details of all study subjects and videos demonstrating the simulation technique are available with the electronic versions of this article on our web site at jbjs.org (go to the article citation and click on "Supplementary Material"). The table is also available on our quarterly CD/DVD (call our subscription department, at 781-449-9780, to order the CD or DVD). ■

NOTE: The authors thank Takeshi Yoshida, MD, Kakuro Denno, MD, Mitsuru Horiki, MD, and Koichi Tada, MD, from the Department of Orthopaedic Surgery, Kansai Rosai Hospital; Kozo Shimada, MD, from the Department of Orthopaedic Surgery, Osaka Koseinenkin Hospital; Shunichi Henmi, MD, from the Department of Orthopaedic Surgery, Ikeda Municipal Hospital; Yoshiharu Nakamura, MD, from the Department of Orthopaedic Surgery, Sakai Municipal Hospital; and Ryoji Nakao, computer programmer, Department of Orthopaedic Surgery, Osaka University Graduate School of Medicine, for their contributions to this study.

Tsuyoshi Murase, MD, PhD
Kunihiro Oka, MD, PhD
Hisao Moritomo, MD, PhD
Akira Goto, MD, PhD
Hideki Yoshikawa, MD, PhD
Kazuomi Sugamoto, MD, PhD
Departments of Orthopaedic Surgery (T.M., K.O., H.M., A.G., and H.Y.) and Orthopaedic Biomaterial Science (K.S.),
Osaka University Graduate School of Medicine, 2-2, Yamada-oka, Suita, Osaka 565-0871, Japan. E-mail address for T. Murase: tmurase-osk@umin.ac.jp. E-mail address for K. Oka: oka-kunihiro@umin.ac.jp. E-mail address for H. Moritomo: moritomo@ort.med.osaka-u.ac.jp. E-mail address for A. Goto: goto-akira@umin.ac.jp. E-mail address for H. Yoshikawa: yhideki@ort.med.osaka-u.ac.jp. E-mail address for K. Sugamoto: sugamoto@ort.med.osaka-u.ac.jp

References

1. Fernandez DL. Malunion of the distal radius: current approach to management. Instr Course Lect. 1993;42:99-113.

2. Fernandez DL. Reconstructive procedures for malunion and traumatic arthritis. Orthop Clin North Am. 1993;24:341-63.

3. Matthews LS, Kaufer H, Garver DF, Sonstegard DA. The effect on supination-pronation of angular malalignment of fractures of both bones of the forearm. J Bone Joint Surg Am. 1982;64:14-7.

4. Sarmiento A, Ebramzadeh E, Brys D, Tarr R. Angular deformities and forearm function. J Orthop Res. 1992;10:121-33.

5. Bilic R, Zdravkovic V, Boljevic Z. Osteotomy for deformity of the radius. Computer-assisted three-dimensional modelling. J Bone Joint Surg Br. 1994;76:150-4.

6. Jupiter JB, Ruder J, Roth DA. Computer-generated bone models in the planning of osteotomy of multidirectional distal radius malunions. J Hand Surg [Am]. 1992;17:406-15.

7. Creasman C, Zaleske DJ, Ehrlich MG. Analyzing forearm fractures in children. The more subtle signs of impending problems. Clin Orthop Relat Res. 1984;188:40-53.

8. Usui M, Ishii S, Miyano S, Narita H, Kura H. Three-dimensional corrective osteotomy for treatment of cubitus varus after supracondylar fracture of the humerus in children. J Shoulder Elbow Surg. 1995;4:17-22.

9. Uchida Y, Ogata K, Sugioka Y. A new three-dimensional osteotomy for cubitus varus deformity after supracondylar fracture of the humerus in children. J Pediatr Orthop. 1991;11:327-31.

10. Brown GA, Firoozbakhsh K, DeCoster TA, Reyna JR Jr, Moneim M. Rapid prototyping: the future of trauma surgery? J Bone Joint Surg Am. 2003;85 Suppl 4:49-55.

11. Ellis RE, Tso CY, Rudan JF, Harrison MM. A surgical planning and guidance system for high tibial osteotomy. Comput Aided Surg. 1999;4:264-74.

12. Perry M, Banks P, Richards R, Friedman EP, Shaw P. The use of computer-generated three-dimensional models in orbital reconstruction. Br J Oral Maxillofac Surg. 1998;36:275-84.

13. Shimizu T, Fujioka F, Gomyo H, Isobe K, Takaoka K. Three-dimensional starch model for simulation of corrective osteotomy for a complex bone deformity: a case report. Foot Ankle Int. 2003;24:364-7.

14. Radermacher K, Portheine F, Anton M, Zimolong A, Kaspers G, Rau G, Staudte HW. Computer assisted orthopaedic surgery with image based individual templates. Clin Orthop Relat Res. 1998;354:28-38.

15. Moritomo H, Murase T, Goto A, Nakajima Y, Masumoto J, Sasama T, Yoshida T, Yachi K. [The usefulness of three dimensional computer simulation for surgical treatment of malunited fracture and nonunion of upper extremities]. J Jpn Soc Surg Hand. 2002;19:252. Japanese.

16. Murase T, Moritomo H, Goto A, Sugamoto K, Yoshikawa H. Does three-dimensional computer simulation improve results of scaphoid nonunion surgery? Clin Orthop Relat Res. 2005;434:143-50.

17. Murase T, Moritomo H, Sugamoto K, Yoshikawa H, Ogata K, Kawasaki K. [3D computer simulation for deformity correction of the limb]. Orthop Surg Traumatol. 2005;48:1055-60. Japanese.

18. Fuller DJ, McCullough CJ. Malunited fractures of the forearm in children. J Bone Joint Surg Br. 1982;64:364-7.

19. Lorensen WE, Cline HE. Marching cubes: a high resolution 3D surface construction algorithm. Comput Graph. 1987;21:163-9.

20. Audette MA, Ferrie FP, Peters TM. An algorithmic overview of surface registration techniques for medical imaging. Med Image Anal. 2000;4:201-17.

21. Beggs JS. Kinematics. Washington: Hemisphere Publishing; 1983. Displacement; p 33-51.

22. Kinzel GL, Hillberry BM, Hall AS Jr, Van Sickle DC, Harvey WM. Measurement of the total motion between two body segments. II. Description of application. J Biomech. 1972;5:283-93.

23. Spoor CW, Veldpaus FE. Rigid body motion calculated from spatial co-ordinates of markers. J Biomech. 1980;13:391-3.

24. Paley D, Herzenberg JE, Tetsworth K, McKie J, Bhave A. Deformity planning for frontal and sagittal plane corrective osteotomies. Orthop Clin North Am. 1994;25:425-65.

25. Paley D. Principles of deformity correction. Berlin: Springer; 2002. p 235-68.

26. Oppenheim WL, Clader TJ, Smith C, Bayer M. Supracondylar humeral osteotomy for traumatic childhood cubitus varus deformity. Clin Orthop Relat Res. 1984;188:34-9.

27. Morrey BF. Anatomy of the elbow joint. In: Morrey BF, editor. The elbow and its disorders. 3rd ed. Philadelphia: WB Saunders; 2000. p 18.